ELSEVIER

The synthesis of multi-walled carbon nanotubes (MWNTs) by catalytic pyrolysis of the phenol-formaldehyde resins

Ioan Stamatin[a], Adina Morozan[a,*], Anca Dumitru[a], V. Ciupina[b],
G. Prodan[b], J. Niewolski[c], H. Figiel[c]

[a]3 Nano-SAE Research Centre, University of Bucharest, MG-38, 077125 Bucharest-Magurele, Romania
[b]Ovidius University of Constantza, Bd. Mamaia 124, Constantza, Romania
[c]Department of Solid State Physics, Faculty of Physics and Applied Computer Science, AGH-University of Science and Technology, 30-059 Krakow, Poland

Abstract

A series of carbon nanomaterials, particularly multi-walled carbon nanotubes (MWNT), are obtained as products from catalytic pyrolysis of the cross-linked phenol-formaldehyde resins with different ferrocene under inert atmosphere. The morphology and structure of the samples were evaluated by TEM and XRD techniques. CNTs morphology is dependent on the iron nanoparticles and their forms (Fe, Fe_3C) resulted from ferrocene decomposition. The amount of nanotubes increases with iron content released from ferrocene catalyst during the pyrolysis process. Fe_3C nanoparticles drive the nucleation and the growth of carbon nanotubes during the pyrolysis process. Long (up to microns) well-defined MWNTs with small defects, ropes and disordered carbon are representatives in the pyrolyzed resins composition.
© 2006 Elsevier B.V. All rights reserved.

1. Introduction

Carbon nanotubes (CNTs), discovered in electric arc-discharge experiments for fullerene synthesis [1], are in the last decade the milestones in the nanotechnology development.

Depending on unique properties, CNTs are attractive materials for a wide range of applications such as nanoelectronics, biosensors [2–5], fillers [6], and gas and energy storage [7]. With the rapidly growing demands of applications in hydrogen storage [8–10] and fuel cells [11,12], there is a major motivation to extend the research on CNTs and composites based on CNTs with tailorable structural, morphological, and surface properties.

Various methods of CNTs synthesis are described in review papers [13,14]. Common for all, either electric arc discharge (EAD), laser ablation (LA), plasma and chemical vapor deposition (CVD), is to reorganize the carbons released from a carbon source in a tube shape via a nanometric transition metal catalyst. Many kinds of organic compounds could be used as carbon source. However, less attention was paid on the catalytic pyrolysis of polymers to synthesize the CNTs. Few works report the conversion of linear polymers (polypropylene, polyethylene and polyvinyl alcohol) in CNTs in the presence of iron-group catalysts [15,16]. An important application of this work is the possibility of large-scale preparation of CNTs from cheap and harmless precursor.

To understand the growing mechanisms of CNTs, the thermodynamic and kinetic approaches are taken into account. The proposed mechanisms by a large number of papers relate the CNTs dimension with catalyst radius, carbon saturation and parameters for synthesis such as temperature, carbon source, and pressure [17,18].

Novolac (phenol-formaldehyde condensation resin) is a good graphene source rising to structures with different shapes when it is simply pyrolyzed. In this context, the aim

*Corresponding author. Tel./fax: +4021 457 48 38.
E-mail address: adina.morozan@gmail.com (A. Morozan).

of our contribution is to present the synthesis of CNTs, with various morphologies and structures, from novolac pyrolysis with different addition of ferrocene up to 900 °C, in an inert atmosphere.

2. Experimental

2.1. Material preparation, preliminary investigations

The resin used as base material was a novolac type (phenol-formaldehyde condensation resin, as received from Romanian company Nitramonia Fagaras). Characteristics: average molecular weight of 670–700 g/mol, phenol content 7%, dropping point 95–105 °C. The cross-linking agent hexamethylenetetramine (HMTA) and ferrocene powder were Merck reagent grade.

The thermal treatment conditions were established by thermo-gravimetric analysis for the composition novolac with 10% HMTA (w/w) dissolved in ethanol, mixed and further dried under vacuum at room temperature. Novolac–HMTA composition was mixed with ferrocene and homogenized in methanol in continuous stirring for 1 h. After the alcohol evaporation for 24 h at 50 °C, the mixtures were minced, sieved on 120 mesh and pressed in pellets. The amount of ferrocene was calculated for 2.5% and 5% by the iron weight to novolac. In terms of the iron content, the samples were indexed as NH-Fe-2.5 and NH-Fe-5. The sample without iron was indexed as NH. The thermo-gravimetry analysis with a heating rate of 20 °C/min up to 800 °C in Ar atmosphere denoted: (1) The optimum temperature for cross-linking: the initial temperature for polymerisation is located in the range of 100–110 °C and the final temperature is in the range of 170–180 °C; (2) the pyrolysis process for cured resins starts around 300 °C. When the temperature reaches 800 °C, a plateau appears indicating the end of pyrolysis process. Carbon yield obtained from the thermo-gravimetric curves was 70%.

2.2. Pyrolyzing process

Based on the preliminary investigations, a very slow pyrolysis process was established as follows:

1. Heating to 180 °C (10 °C/min) in air, 1 h soaking time to produce a large cross-linked lattice.
2. Heating to 300 °C for 1 h in Ar atmosphere, 30 min soaking time which is close to initiate pyrolysis and ferrocene decomposition.
3. Pyrolysis regime from 300 to 900 °C, at rate of 3 °C/min.
4. At 900 °C, samples were kept for 1 h, and then free cooled to room temperature.

To find the influence of the thermal treatment to the structural changes, we repeat the experiment for NH-Fe-5 increasing the heating rate of the third pyrolysis step from 3 to 10 °C/min.

2.3. Characterization

The morphology and structure of samples were investigated using transmission electron microscopy (TEM) and X-ray diffraction (XRD). Philips CM120ST (Customized Microscope 120 Super Twin) was used for collecting the TEM images. XRD patterns were registered in a Siemens D5005 diffractometer, using CuK_α radiation ($\lambda = 1.5406$ Å), (40 kV and 45 mA conditions). Data were collected over the 2θ range of 5–120°, 0.025° steps and 16 s counting time per step.

3. Results and discussions

For lower iron content, NH-Fe-2.5, the predominant features in TEM images is the formation of nanoparticles surrounded by graphene sheets and not many events with nanotubes development (Figs. 1a and b). Iron nanoparticles resulted from ferrocene decomposition appear as ellipsoids and clusters (Fig. 1a). With the increase in iron content, NH-Fe-5, large and long structures of MWNTs are observed (Figs. 2a and b).

The morphology of the carbon materials that resulted from pyrolysis process shows ropes structures (Fig. 2c) beside regular MWNTs with different level of defects (Fig. 2d). Moreover, in the Fig. 2d the outside diameter, the inner diameter and the distance between graphene sheets of MWNTs are presented.

The most interesting aspect in TEM picture (Fig. 3b) is the tendency of the graphene to bend around the iron nanoparticles in the case of NH-Fe-5 (fast heating rate). This tendency was also observed in the case of NH-Fe-5 (lower heating rate), Fig. 2c. It is not clear, if the aromatic rings can rotate to each other or they are ropes as whole. If the roping is as a whole, then they are simple nanotubes bundles. If the aromatic rings are rotating with 90° to each other, then we can show by modeling that a spiro-graphene (Fig. 4a) and a possible carbon nanotube such as hypothetical spiro-nanotube can be obtained (Fig. 4b).

Referring to iron nanoparticles and the mechanism of developing CNTs, in Fig. 3b it is observed that the graphene sheets are developed parallel with crystalline plane. The graphene growth is distorted at the corner between two planes. When the crystallographic plane is changed, the graphene sheets change morphology by rotation with 90°. Here, it is possible to get spiro-structure, and to develop by chance spiro-nanotube as in Fig. 4.

The XRD patterns of as prepared samples NH, NH-Fe-2.5 and NH-Fe-5 are shown in Fig. 5. It is well known that a typical carbon structure obtained at low temperatures (500–1200 °C) exhibits a XRD pattern consisting of a few broad bands located near the (0 0 2), (1 0 0), (1 1 0) and (1 1 2) reflections of graphite. The prominent peak about $2\theta = 26°$ can be attributed to the (0 0 2) reflection of carbon. A typically carbon amorphous structure is obtained in the case of NH.
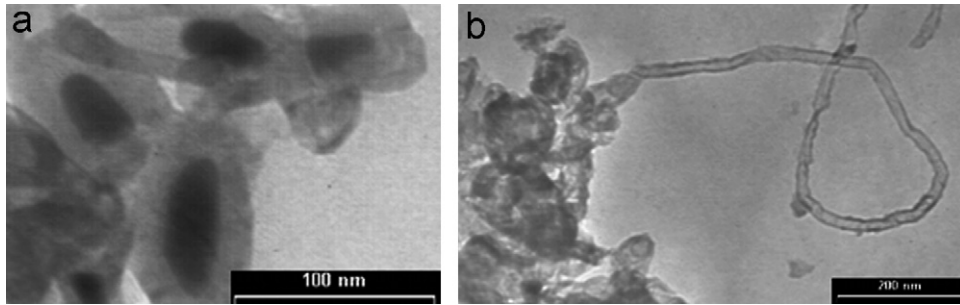
Fig. 1. (a) NH-Fe-2.5: ellipsoid iron nanoparticles; (b) CNT developed from NH-Fe-2.5.
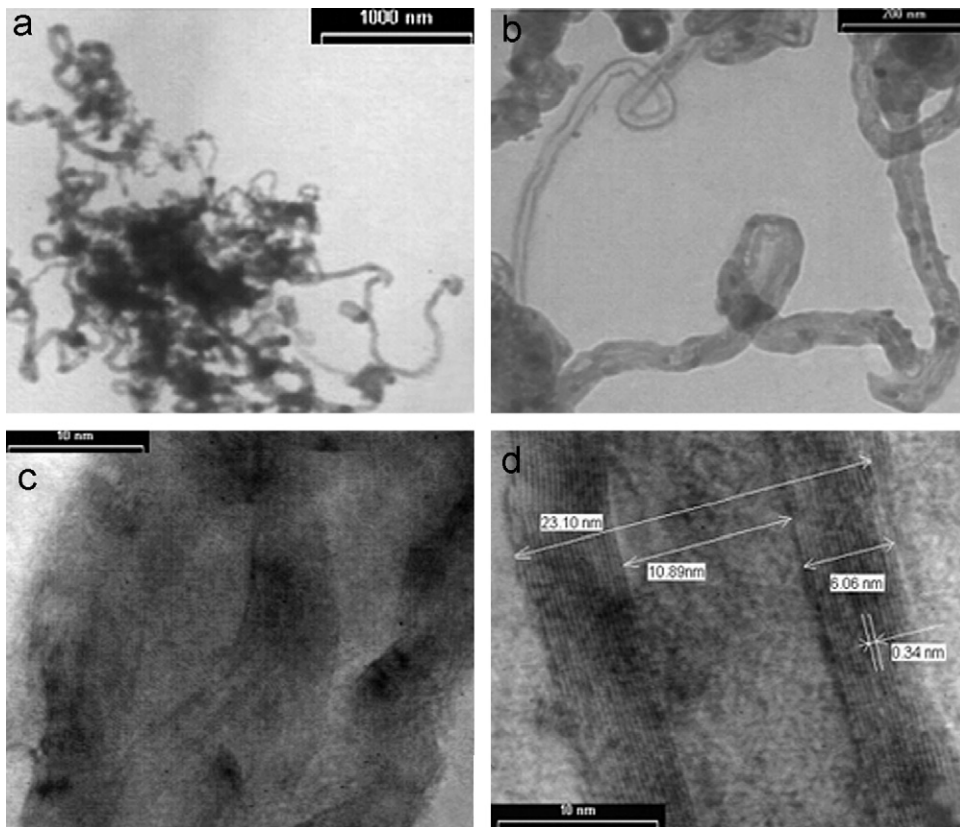
Fig. 2. (a), (b) MWNTs and rope structure from NH-Fe-5; (c), (d) details of rope structure and MWNTs of NH-Fe-5.
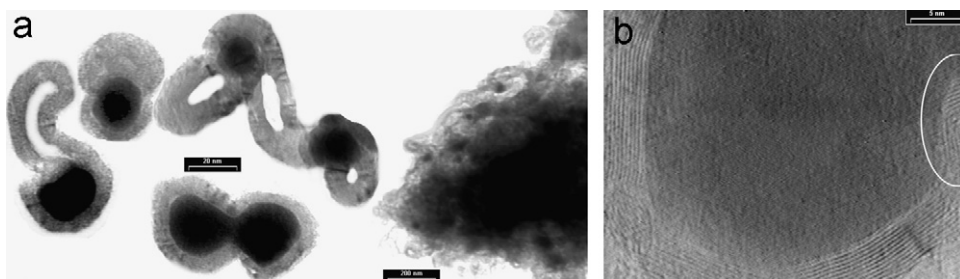
Fig. 3. (a) Graphenes sheets developed around iron nanoparticles for NH-Fe-5 (fast heating). (b) The graphenes growth near to nanoparticles interface. Different crystallographic plane induces a specific disposal of the graphenes.
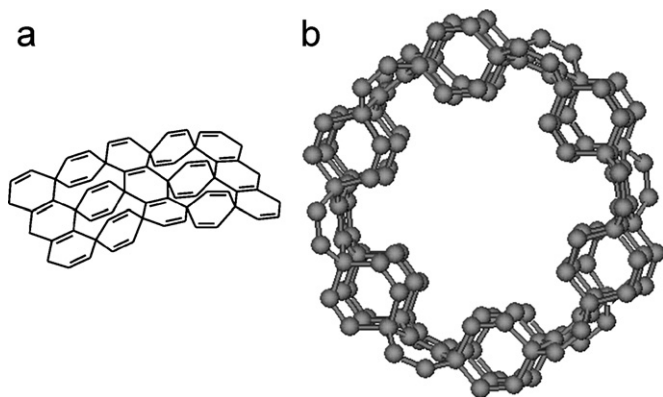
Fig. 4. Spiroconjugation aspects: (a) spiro-graphene; (b) spiro-nanotube.
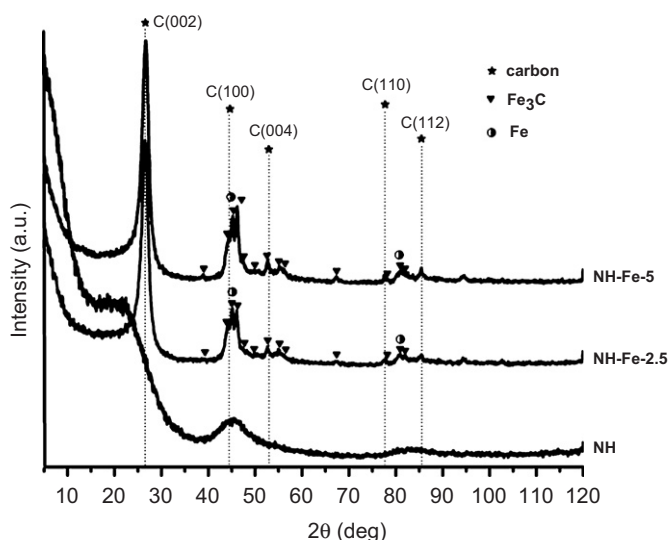
Fig. 5. XRD patterns for NH, NH-Fe-2.5 and NH-Fe-5 samples. The peaks corresponding to MWNTs and the second phases, Fe₃C and Fe are indexed.

The d_{002} values derived from this XRD patterns are 3.366 Å (NH-Fe-2.5 and $2\theta = 26.46°$), and respectively, 3.357 Å (NH-Fe-5 and $2\theta = 26.53°$), which are slightly higher than that of the perfect graphite ($d_{002} = 3.354$ Å). The degree of graphitization (g) was calculated based on the Maire and Mering formula [19] and the calculated number of walls from MWNTs ($n = L_c/d_{002} \sim 14$, where L_c are estimated from the width of the (002) Bragg line using the Debye–Scherrer formula) corresponds with TEM analysis. The synthesized CNTs are not totally graphitized; g is 85.34% for NH-Fe-2.5 and 95.58% for NH-Fe-5, but the degree of graphitization increase with ferrocene content.

XRD measurements indicate that beside the CNTs, the main phases are Fe₃C that is known to be an active phase for the CNTs formation [20,21] and Fe. The diffraction peaks associated with Fe₃C and Fe phases, indexed in Fig. 4, are in agreement with other reports [22,23].

These results bring a supplement of data to the understanding of the growing mechanisms of CNTs synthesis from polymer pyrolysis. The catalytic surface is a metal cluster with few nanometers radius and the graphenes resulting from a supersaturated solution start to nucleate and grow in a nanotube shape. In consequence, a system rich in carbon source embedded with nanometer catalyst and in suitable conditions of temperature and pressure will nucleate and grow nanotube species by graphene's reorganization. These mechanisms do not take into account the composition of iron nanoparticles that can be Fe, Fe₃C or an alloy. In our results, it was observed that the amount of iron compounds beside a suitable regime in temperature and pressure is important to promote the nanotube growth.

4. Conclusions

The pyrolysis of the polymers containing aromatic rings, for instance novolac cured with HMTA, without iron content rise to regular amorphous carbon. When the iron nanoparticles released from ferrocene decomposition, the pyrolysis process develop MWNTs and other structures such as ropes. The graphenes are formed by carbon reorganization on the iron nanoparticles surface by complex mechanisms of diffusion-transport and reorganization at atomic level. The morphology of resulting carbon structure is dependent on iron content and heating rate of pyrolysis process. Disordered and not well-developed CNTs are observed at high heating rate (10 °C/min). Long and large CNTs beside ropes and possible strange structures of spiro-graphenes and spiro-nanotubes are developing under low heating rate (3 °C/min). The composition and the level of organization of the iron nanoparticles and the nature of the crystallographic plane in contact with graphene are determinant for CNTs growth with fewer defects.

Nanometer iron resulting from ferrocene decomposition is formed by iron atoms clusterizing induced by diffusion processes and reactions in the solid state. The presence of iron in pyrolyzed system leads to the obtaining of carbon structures similar with nanotubes, in our case MWNTs.

References

[1] S. Iijima, Nature 354 (1991) 56.
[2] S.J. Tans, A.R.M. Verschueren, C. Dekker, Nature 393 (1998) 49.
[3] H. Dai, J.H. Hafner, A.G. Rinzler, D.T. Colbert, R.E. Smalley, Nature 384 (1996) 147.
[4] J. Kong, N.R. Franklin, C. Zhou, M.G. Chapline, S. Peng, K. Cho, H. Dai, Science 287 (2000) 622.
[5] Y. Nakayama, S. Akita, Synth. Met. 117 (2001) 207.
[6] K.T. Lau, D. Hui, Composites B 33 (2002) 263.

[7] G.X. Wang, J.-H. Ahn, J. Yao, A. M. Lindsay, H.K. Liu, S.X. Dou, J. Power Sour. 119–121 (2003) 16.

[8] S.M. Lee, K.S. Park, Y.C. Choi, Y.S. Park, J.M. Bok, D.J. Bae, K.S. Nahm, Y.G. Choi, S.C. Yu, N.-G. Kim, T. Frauenheim, Y.H. Lee, Synth. Met. 113 (2000) 209.

[9] H.-M. Cheng, Q.-H. Yang, C. Liu, Carbon 39 (2001) 1447.

[10] P.-X. Hou, S.-T. Xu, Z. Ying, Q.-H. Yang, C. Liu, H.-M. Cheng, Carbon 41 (2003) 2471.

[11] R.P. Raffaelle, B.J. Landi, J.D. Harris, S.G. Bailey, A.F. Hepp, Mater. Sci. Eng. B 116 (2005) 233.

[12] M. Carmo, V.A. Paganin, J.M. Rosolenb, E.R. Gonzalez, J. Power Sources 142 (2005) 169.

[13] J, Liu, S. Fan, H. Dai, MRS Bull. 29 (4) (2004) 244.

[14] C. Journet, P. Bernier, Appl. Phys. A. 67 (1998) 1.

[15] Y.-H. Chung, S. Jou, Mater. Chem. Phys. 92 (2005) 256.

[16] N.I. Maksimova, O.P. Kirvoruchko, G. Mestl, V.I. Zaikovskii, A.L. Chuvilin, A.N. Salanov, E.B. Burgina, J. Mol. Catal. A 158 (2000) 301.

[17] V.L. Kuznetsov, A.N. Usoltseva, A.L. Chuvilin, E.D. Obraztsova, J.-M. Bonard, Phys. Rev. B 64 (23) (2001) 5401.

[18] V.L. Kuznetsov, in: S. Guceri, Y.G. Gogotsi, V. Kuznetsov, (Eds.), NATO Science Series, vol.169, 2003. p. 19.

[19] M.A. Ermakova, D.Y. Ermakov, A.L. Chuvilin, G.S. Kuvshinov, J. Catal. 201 (2001) 183.

[20] M. Perez-Cabero, I. Rodriguez-Ramos, A. Guerrero-Ruiz, J. Catal. 215 (2003) 305.

[21] J.W. Snoeck, G.F. Froment, M. Fowles, J. Catal. 169 (1997) 240.

[22] S. Liu, R.J. Wehmschulte, Carbon 43 (2005) 1550.

[23] C. Emmenegger, J.M. Bonard, P. Mauron, P. Sudan, A. Lepora, B. Grobety, A. Zuttel, L. Schlapbach, Carbon 41 (2003) 539.